Structural Changes of *Salinibacter* Sensory Rhodopsin I upon Formation of the K and M Photointermediates[†]

Daisuke Suzuki,[‡] Yuki Sudo,[‡] Yuji Furutani,[§] Hazuki Takahashi,[§] Michio Homma,[‡] and Hideki Kandori*[,§]

Division of Biological Science, Graduate School of Science, Nagoya University, Chikusa-ku, Nagoya, 464-8602, Japan, and Department of Frontier Materials, Nagoya Institute of Technology, Showa-ku, Nagoya, 466-8555, Japan

Received July 19, 2008; Revised Manuscript Received September 23, 2008

ABSTRACT: Sensory rhodopsin I (SRI) is one of the most interesting photosensory receptors in nature because of its ability to mediate opposite signals depending on light color by photochromic one-photon and two-photon reactions. Recently, we characterized SRI from eubacterium *Salinibacter ruber* (*Sr*SRI). This protein allows more detailed information about the structure and structural changes of SRI during its action to be obtained. In this paper, Fourier transform infrared (FTIR) spectroscopy is applied to *Sr*SRI, and the spectral changes upon formation of the K and M intermediates are compared with those of other archaeal rhodopsins, SRI from *Halobacterium salinarum* (*Hs*SRI), sensory rhodopsin II (SRII), bacteriorhodopsin (BR), and halorhodopsin (HR). Spectral comparison of the hydrogen out-of-plane (HOOP) vibrations of the retinal chromophore in the K intermediates shows that extended choromophore distortion takes place in *Sr*SRI and *Hs*SRI, as well as in SRII, whereas the distortion is localized in the Schiff base region in BR and HR. It appears that sensor and pump functions are distinguishable from the spectral feature of HOOP modes. The HOOP band at 864 cm^{-1} in SRII, important for negative phototaxis, is absent in *Sr*SRI, suggesting differences in signal transfer mechanism between SRI and SRII. The strongly hydrogen-bound water molecule, important for proton pumps, is observed at 2172 cm^{-1} in *Sr*SRI, as well as in BR and SRII. The formation of the M intermediate accompanies the appearance of peaks at 1753 (+) and 1743 (−) cm^{-1}, which can be interpreted as the protonation signal of the counterion (Asp72) and the proton release signal from an unidentified carboxylic acid, respectively. The structure and structural changes of *Sr*SRI are discussed on the basis of the present infrared spectral comparisons with other rhodopsins.

Microorganisms respond and adapt to various environmental stimuli. They show attractant and repellent responses (taxis) to survive in various environments where they are living. Taxis to chemicals including to some amino acids, temperature, pH, and light is known as chemotaxis, thermotaxis, pH-taxis, and phototaxis, respectively (*1*). The archaeon *Halobacterium salinarum* has two photoreceptors regulating negative and positive phototaxis. One of them, sensory rhodopsin I (SRI)[1]works as a dual receptor both for negative and positive phototaxis (*2*). Sensory rhodopsin II (SRII, also known as phoborhodopsin, pR) is a negative phototaxis receptor in the cells (*3*). SRI and SRII form 2:2 complexes with their transducer proteins, halobacterial transducer protein I for SRI (HtrI) and halobacterial transducer protein II for SRII (HtrII) (*4, 5*), and transmit light signals to a two-component signal transduction cascade, which controls the flagella motor rotation (*6*).

SRI is one of the most interesting photosensory receptors in nature because of its novel ability to mediate opposite signals depending on light color by photochromic one- and two-photon reactions (*2, 7*). However, the molecular mechanism of SRI is not understood in atomic terms. On the other hand, the signal relay mechanism of SRII is well characterized by using various methods because SRII from *Natronomonas pharaonis* (*Np*SRII) has high stability in dilute salt solutions and is much more resistant against detergents (*8, 9*), whereas *Hs*SRI is unstable in those conditions. Recently, we characterized an extremely stable SRI-like protein from a eubacterium *Salinibacter ruber*, which was named *Sr*SRI (*10*). This protein is the first eubacterial SRI as a functional protein. *Sr*SRI has an all-*trans* retinal as a chromophore with an absorption maximum at 558 nm and shows a slow photocycle. These properties are close to those of *Hs*SRI. *Sr*SRI is highly stable within the membrane and in detergent micelles even in the absence of NaCl. In addition, a functional expression system utilizing *Escherichia coli* cells can provide a large amount of the proteins (*10*).

Besides SRI and SRII, *H. salinarum* has two other retinal proteins, bacteriorhodopsin (BR) and halorhodopsin (HR),

[†] This work was supported by grants from Japanese Ministry of Education, Culture, Sports, Science, and Technology to Y.S. (No. 20050012), to Y.F. (No. 19045015), and to H.K. (Nos. 19370067 and 20050015).

* To whom correspondence should be addressed. Phone and Fax: 81-52-735-5207. E-mail: kandori@nitech.ac.jp.

[‡] Nagoya University.

[§] Nagoya Institute of Technology.

[1] Abbreviations: *Sr*SRI, sensory rhodopsin I from *Salinibacter ruber*; FTIR, Fourier transform infrared; $SrSRI_K$, K-intermediate of *Sr*SRI; $SrSRI_M$, M-intermediate of *Sr*SRI; *Hs*SRI, sensory rhodopsin I from *Halobacterium salinarum*; BR, light-adapted bacteriorhodopsin from *Halobacterium salinarum*; HR; halorodopsin from *Natronomonas pharaonis*; SRII, sensory rhodopsin II from *Natronomonas pharaonis*; BR-T, P200T/V210Y/A215T triple mutant of BR; HOOP, hydrogen out-of-plane.

10.1021/bi801358b CCC: $40.75
Published on Web 11/08/2008

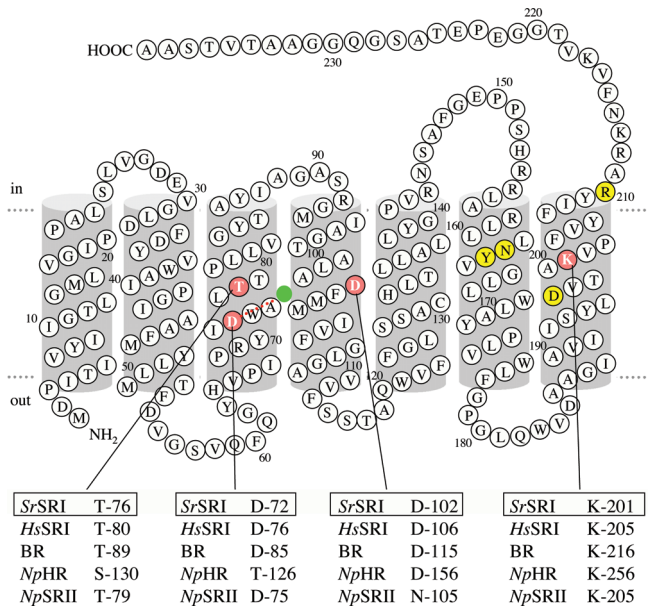

FIGURE 1: Predicted secondary structure of *Salinibacter ruber* sensory rhodopsin I (*Sr*SRI). Names of the other rhodopsins are *Hs*SRI, sensory rhodopsin I from *Halobacterium salinarum*; BR, bacteriorhodopsin from *Halobacterium salinarum*; *Np*HR, halorhodopsin from *Natronomonas pharaonis*; and *Np*SRII, sensory rhodopsin II from *Natronomonas pharaonis.* Amino acid residues colored with yellow are necessary for function in *Hs*SRI. The N165F, H166Y, and D201N mutations convert the normally attractant signal to a repellent signal (*7, 60, 61*). The R215W is a suppressor mutation (*62*). We focused on the residues colored pink. A strongly hydrogen-bonded water molecule is shown as a filled green circle.

which work as light-driven ion pumps, whose functions are distinctly different from those of SRI and SRII. Namely, BR and HR function as a light-driven outward proton pump and a light-driven inward chloride pump, respectively. The original state of SRI (λ_{max} = 587 nm) and its long-lived photointermediate (the M-intermediate; λ_{max} = 373 nm) are important for positive and negative phototaxis, respectively (*6*). SRII is a negative phototaxis receptor in haloarchaea, including *H. salinarum* and *N. pharaonis*. Those are called *Hs*SRII and *Np*SRII, respectively, and their absorption maxima are at about 500 nm (*8*). Thus, haloarchaea are attracted to light with wavelengths longer than 520 nm, and they avoid light with wavelengths shorter than 520 nm due to the functions of SRI and SRII (*6*). Light at >520 nm can activate the ion pumping rhodopsins (BR and HR) to obtain light-energy, and cells avoid light of shorter wavelengths, which contains harmful near-UV. Interestingly it was reported that SRI and SRII are able to function as an outward proton pump like BR only in the absence of the cognate transducer proteins (*11, 12*), suggesting that these retinal proteins mentioned above are presumably evolved from the same protein and have similar structures (Figure 1). In fact, the rhodopsins have seven transmembrene helices and a retinal chromophore bound to a specific lysine residue of helix G via a protonated Schiff base linkage (*13*). To stabilize the positive charge of a protonated Schiff base inside the protein, highly conserved charged groups are present in the Schiff base region: arginine and aspartate of helix C and aspartate of helix G. Water molecules also stabilize the charged group in the region (*13*). In particular, three water molecules are involved in the pentagonal cluster structure (*14, 15*). A strongly hydrogen-bound water molecule located between the Schiff base and the counterion exists in the light-driven proton pumps, BR (*16*), transducer-free SRII (*17*), HR with azide (*18*), and D212N BR mutant with NaCl (*19*). Thr204 in SRII located around the retinal chromophore (The distance from the C14 atom to the hydroxyl oxygen of Thr204 is 4.4 Å.) is quite an important residue for negative phototaxis (*15, 20*). Thus, structural changes of the Schiff base region and internal water molecules are directly linked to functions of retinal proteins.

Light absorption of these retinal proteins triggers a cyclic reaction that is comprised of a series of intermediates, designated alphabetically (*21*). The *trans*−*cis* photoisomerization of the retinal chromophore leads to the formation of the K intermediate. In proton pumps, the primary proton transfer takes place in the L to M transition. A proton is transferred from the protonated Schiff base (Lys205 for *Hs*SRI; Lys216 for BR; Lys205 for SRII) to an aspartate of helix C (Asp76 for *Hs*SRI; Asp85 for BR; Asp75 for SRII). In BR, a proton is released simultaneously from a protonated water cluster to the extracellular side (*22, 23*). Consequently the proton was transferred from the cytoplasmic side to the extracellular side. Thus, the molecular properties of ion-pumping rhodopsins, especially BR, have been extensively studied.

How about photosensory rhodopsins? SRII has been well-characterized over the past several years using various methods because of its high protein stability (*24*). The crystallographic structure of SRII and the SRII/HtrII complex had been achieved (*5, 15*), and light-induced structural changes were also identified by various methods, including UV−vis, electron paramagnetic resonance (EPR) spectroscopy, etc. Interestingly, the structure and structural changes are almost the same as those of BR, implying that the functional differentiation was caused by small structural differences in some amino acid side chain(s) or main chain(s). In fact, Sudo and Spudich recently reported that substitution of only three residues, P200T/V210Y/A215T, converted BR into a sensor for negative phototaxis like SRII (BR-T), indicating similar structural changes between BR and SRII (*25*). On the other hand, little is known about the molecular mechanism(s) of interactions between SRI and HtrI, about structural changes, or about the signal relay mechanism of positive phototaxis.

Here, we utilized Fourier transform infrared (FTIR) spectroscopy to explore structural changes of *Sr*SRI. FTIR spectroscopy is a powerful tool to investigate structure−function relationship in rhodopsins. In the case of SRII, a transducer-dependent specific interaction of Thr204 was first found (*26*), followed by phototaxis analysis revealing the important role of Thr204 in function (*20*). Then, the origin of such a specific interaction related to Thr204 was revealed from a positive correlation between the increment of a retinal vibration in the K intermediate and the physiological phototaxis response (*27, 28*). In *Hs*SRI, earlier studies identified characteristic vibrational bands such as Asn53 (*29*) and Asp76 (*30*). It was also shown that $Hs\text{SRI}_M$ contains 13-*cis* retinal (*31*). Hydrated film samples of *Sr*SRI were stable in the absence of salt, in contrast to *Hs*SRI (*32*). This enabled us to obtain accurate light-induced difference spectra upon formation of the K and M intermediates in the entire mid-infrared region. In this study, we report light-induced

difference FTIR spectra at neutral pH, where the Schiff base counterion (Asp72) is deprotonated. The obtained spectra for *Sr*SRI are compared with those of other archaeal rhodopsins such as BR, HR, *Hs*SRI, and SRII.

MATERIALS AND METHODS

Preparation of SrSRI and HsSRI Samples. SrSRI and *Hs*SRI were prepared as described previously (*10, 32, 33*). Briefly, the *Sr*SRI and *Hs*SRI proteins with a six-histidine tag at the C-terminus were expressed in *E. coli* BL21(DE3) cells, solubilized with 1.0% *n*-dodecyl β-D-maltoside (DDM), and purified with a Ni^{2+}-NTA column (QIAGEN, Valencia, CA, USA) as described previously (*34*). Purified samples were then reconstituted into L-α-phosphatidylglycerol (PG) liposomes (SRI/PG = 1:50 molar ratio) by removing the detergent with Bio-Beads (SM2, Bio-Rad, Hercules, CA).

FTIR Spectroscopy. Low-temperature FTIR spectroscopy was performed with 2-cm^{-1} resolution as described previously (*17*). The *Sr*SRI samples in PG liposomes were washed with a 2 mM phosphate buffer (pH 7.0). Then a 90 μL aliquot of the sample (0.1−1 mg) was dried on a BaF_2 window with a diameter of 18 mm. The *Hs*SRI samples in PG liposomes were washed with a 15 mM borate buffer (pH 8.3) containing 300 mM NaCl. Then a 40 μL aliquot of the sample (0.1−1 mg) was dried on a BaF_2 window with a diameter of 18 mm, and deposition of excess salt was washed away with a 15 mM borate buffer (pH 8.3) containing 15 mM NaCl. After hydration with H_2O, D_2O, or $D_2{}^{18}O$, the sample was placed in a cell, which was mounted in an Oxford DN-1704 cryostat equipped in the Bio-Rad FTS-40 spectrometer.

The *Sr*SRI_K minus *Sr*SRI difference spectra were measured at 77 K as follows. Illumination of the *Sr*SRI film with a 450 nm light for 2 min at pH 7.0 and 77 K converted *Sr*SRI to *Sr*SRI_K, and subsequent illumination with >640 nm light forced *Sr*SRI_K to revert to *Sr*SRI. The *Sr*SRI_M minus *Sr*SRI difference spectra were measured at 260 K and pH 7.0 as follows. To convert *Sr*SRI to *Sr*SRI_M, the sample was irradiated with >480 nm light for 2 min, after which subsequent 1 min illumination with UV light changed *Sr*SRI_M back to *Sr*SRI. The difference spectrum was calculated from the spectra constructed with 128 interferograms before and after the illumination. Twenty-four or sixteen spectra obtained in this way were averaged for the *Sr*SRI_K minus *Sr*SRI or *Sr*SRI_M minus *Sr*SRI spectra. The *Hs*SRI_K minus *Hs*SRI difference spectra were measured at 77 K. Illumination of the *Hs*SRI film with 500 nm light for 2 min at pH 7.0 and 77 K converted *Sr*SRI to *Sr*SRI_K, and subsequent 1 min illumination with >680 nm light forced *Hs*SRI_K to revert to *Hs*SRI.

BR_K minus BR, HR_K minus HR, $SRII_K$ minus SRII, BR-T_K minus BR-T spectra, BR_M minus BR, *Hs*SRI_M minus *Hs*SRI, and $SRII_M$ minus SRII spectra were taken from Shibata et al. *(35)*, Shibata et al. *(36)*, Kandori et al. *(34)*, Sudo et al. *(37)*, Tanimoto et al. *(38)*, Furutani et al. *(32)*, and Furutani et al. *(39)*, respectively. All spectra were normalized with respect to the C−C or C═C stretching vibration of the retinal chromophore.

RESULTS

Infrared Spectral Changes of SrSRI and HsSRI upon Formation of K Photointermediate. Figure 2a,b shows the K minus initial state difference FTIR spectra of *Sr*SRI and *Hs*SRI, respectively. The $SRII_K$ minus SRII (Figure 2c) is reproduced from ref *34* for comparison. The spectrum of *Hs*SRI was too noisy at <872 cm^{-1} because of scattering, so that the region was removed. The bands at 1527 (−)/1516 (+) cm^{-1} for *Sr*SRI, 1529 (−)/1518 (+) cm^{-1} for *Hs*SRI, and 1554 (−)/1544 (+) cm^{-1} for SRII correspond to the ethylenic C═C stretching vibrations of the retinal chromophore. The lower frequency shift corresponds to the spectral red-shift upon formation of the K intermediate. The bands at 1250 (−), 1200 (−), 1192 (+), and 1165 (−) cm^{-1} for *Sr*SRI, 1249 (−), 1199 (−), 1191 (+), and 1163 (−) cm^{-1} for *Hs*SRI, and 1244 (−), 1203 (−), and 1198 (+) cm^{-1} for SRII correspond to the C−C stretching vibrations of the retinal chromophore, and the frequency shift represents retinal isomerization from the all-*trans* to 13-*cis* form. Thus, these results indicate the formation of the K intermediate both in *Sr*SRI and *Hs*SRI as well as in SRII. Negative bands were observed at 1165 cm^{-1} for *Sr*SRI and 1163 cm^{-1} for *Hs*SRI, but not for SRII. It is likely that the bands originate from C10−C11 stretching vibration, because the corresponding band of BR appears at 1170 cm^{-1} and is assigned to C10−C11 stretching vibration (*40*).

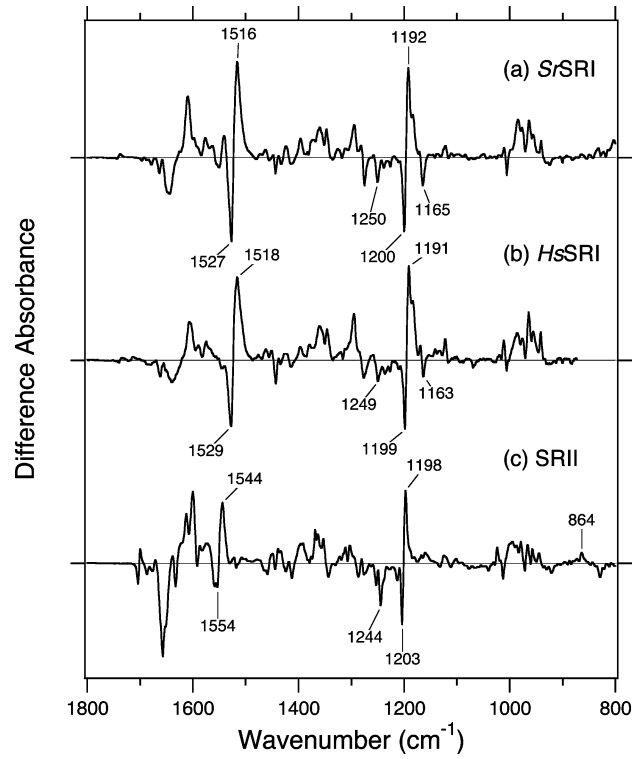

FIGURE 2: *Sr*SRI_K minus *Sr*SRI (a) and *Hs*SRI_K minus *Hs*SRI (b) difference infrared spectra measured at 77 K at pH 7.0 and 8.5, respectively, in the 1800−800 cm^{-1} region. The spectrum of *Hs*SRI is deleted at <872 cm^{-1}. The *Hs*SRI_K minus *Hs*SRI spectrum (b) is multiplied by 4.2 for sake of comparison. The samples were hydrated with H_2O. The $SRII_K$ minus SRII difference FTIR spectrum (c) is reproduced from ref *34* for comparison. One division of *y* axis corresponds to 0.018 absorbance units.

Figure 3 shows the spectral changes in the 1780−1560 cm^{-1} region, where most signals originate from vibrations of protein. One exception is the C═N stretching vibration of the retinal Schiff base. Among various D_2O sensitive bands of SRII (c), the C═N stretch has been assigned at 1650 cm^{-1} in H_2O and 1633 cm^{-1} in D_2O (*34*). The 1646 and 1622 cm^{-1} bands for *Sr*SRI are tentatively assigned to the C═N stretches of the retinal Schiff base in H_2O and D_2O,

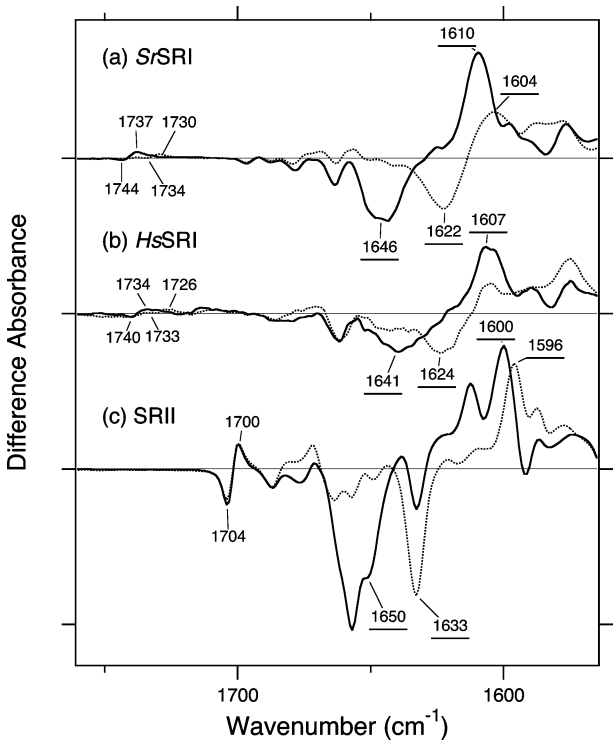

FIGURE 3: *Sr*SRI$_K$ minus *Sr*SRI (a) and *Hs*SRI$_K$ minus *Hs*SRI (b) difference infrared spectra measured at pH 7.0 and 8.5, respectively, in the 1780−1565 cm^{-1} region. The *Hs*SRI$_K$ minus *Hs*SRI spectra are multiplied by 4.2 for sake of comparison. The samples were hydrated with H_2O (—) or D_2O (•••). Underlined values correspond to C═N stretching vibration. The SRII$_K$ minus SRII difference FTIR spectra (c) are reproduced from ref *34* for comparison. One division of *y* axis corresponds to 0.008 absorbance units.

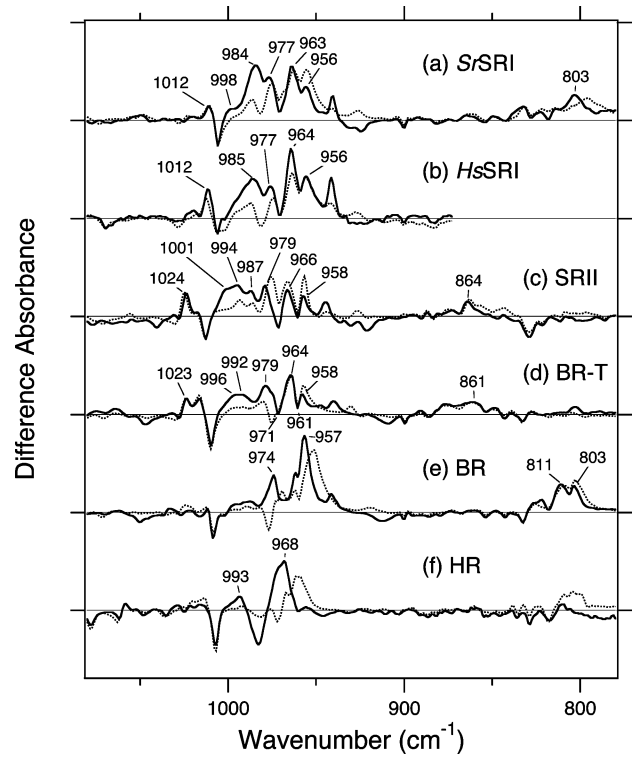

FIGURE 4: *Sr*SRI$_K$ minus *Sr*SRI (a) and *Hs*SRI$_K$ minus *Hs*SRI (b), difference infrared spectra measured at pH 7.0 and 8.5, respectively, in the 1080−780 cm^{-1} region. The spectrum of *Hs*SRI was deleted at <872 cm^{-1}. The *Hs*SRI$_K$ minus *Hs*SRI spectra are multiplied by 4.2 for sake of comparison. The samples were hydrated with H_2O (—) or D_2O (•••). The SRII$_K$ minus SRII (c), BR-T$_K$ minus BR-T (d), BR$_K$ minus BR (e), and HR$_K$ minus HR (f) difference FTIR spectra are reproduced from refs *34*, *37*, *35*, and *36*, respectively, for comparison. One division of *y* axis corresponds to 0.006 absorbance units.

respectively. Previous resonance Raman of *Hs*SRI reported those frequencies at 1634 and 1616 cm^{-1} (*31*). Therefore, the 1641 and 1624 cm^{-1} bands in Figure 3b probably originate from the Schiff base C═N stretches of *Hs*SRI in H_2O and D_2O, respectively. The spectral upshift in H_2O is caused by the coupling of the N−H bending vibration of the Schiff base, and the difference in frequency between H_2O and D_2O has been regarded as the marker of hydrogen-bonding strength of the Schiff base nitrogen. Frequency differences in *Sr*SRI (1646 − 1622 = 24 cm^{-1}) and *Hs*SRI (1641 − 1624 = 17 cm^{-1}) are similar to the value in SRII (1650 − 1633 = 17 cm^{-1}), indicating that the hydrogen-bonding strengths of the Schiff base in SRIs are similar to that of SRII. In the K state, the C═N stretching vibrations appear at 1610−1600 cm^{-1}, though the band in D_2O is unclear only for *Hs*SRI (Figure 3b).

In SRII, the 1704 (−)/1700 (+) cm^{-1} bands were assigned as the C═O stretching vibration of Asn105, and the strong peaks are characteristic for SRII (*41*). Corresponding amino acids are Asp102 in *Sr*SRI and Asp106 in *Hs*SRI. In *Sr*SRI and *Hs*SRI, the 1744 (−)/1737 (+) and 1740 (−)/1734 (+) cm^{-1} bands in H_2O shifted to 1734 (−)/1730 (+) and 1733 (−)/1726 (+) cm^{-1} in D_2O (Figure 2a,b), respectively. They were ascribable to the C═O stretching vibrations of Asp102 for *Sr*SRI and Asp106 in *Hs*SRI, respectively. The corresponding bands appear at 1742 (−)/1733 (+) cm^{-1} in BR and 1744 (−)/1737 (+) cm^{-1} in HR (*41*−*43*), and their intensities are similar to those of *Sr*SRI and *Hs*SRI. It should be noted that the carboxylic C═O stretch of the N105D mutant SRII exhibits intense bands at 1744(−)/1739(+) cm^{-1} in H_2O and at 1734(−)/1728(+) cm^{-1} in D_2O (*41*). Thus, the structure and structural changes at position 102 in *Sr*SRI (106 in *Hs*SRI) are similar to those of ion-pumping rhodopsins.

Figure 4 shows spectral changes in the 1080−780 cm^{-1} region, where hydrogen out-of-plane (HOOP) vibrations of the retinal molecule are mainly observed. Difference FTIR spectra for SRII (c), BR-T (d), BR (e), and HR (f) are reproduced from refs *34*, *37*, *35*, and *36*, respectively, for comparison. The *Sr*SRI$_K$ minus *Sr*SRI and the *Hs*SRI$_K$ minus *Hs*SRI spectra exhibit intense positive peaks at 998, 984, 977, 963, and 956 cm^{-1} for *Sr*SRI, and at 985, 977, 964, and 956 cm^{-1} for *Hs*SRI, which would be tentatively assigned to HOOP vibrations of the retinal chromophore. These results suggest that the structural changes spread to the middle part of the retinal chromophore in SRI. By using all seven monodeutrated retinal analogues, Furutani et al. assigned the 966 (+)/971 (−) and 958 (+)/961 (−) cm^{-1} bands in SRII as the C7═C8 and C11═C12 Au (irreducible representation of diene vibrations) HOOP modes, respectively, and the positive bands at 1001, 994, 987, and 979 cm^{-1} as the C15-HOOP vibrations (*40*). From the similarity in frequency, the bands at 998, 984, and 977 cm^{-1} in *Sr*SRI are likely to originate from C15-HOOP (Figure 4a). The bands at 963 and 956 cm^{-1} are likely to originate from C7═C8 and C11═C12 Au HOOP vibration, respectively. These bands were also observed in a BR mutant engineered to transmit photosensory signals like SRII (BR-T) at 964 (+)/971 (−), 958 (+)/961 (−), 996 (+), 992 (+), and 979

(+) cm^{-1} (Figure 4d), implying the importance of the extended chromophore distortion for phototaxis signaling. In addition, a positive band at 1012 cm^{-1} appears both in *Sr*SRI$_K$ and *Hs*SRI$_K$. A similar band is also present at 1024 cm^{-1} in SRII$_K$ and at 1023 cm^{-1} in BR-T$_K$, which was assigned to symmetric rocking of methyl groups connected to the C9 and C13 atoms (*37, 40*).

On the other hand, only two intense positive peaks were observed for ion-pumping rhodopsins, at 974 and 957 cm^{-1} for BR (Figure 4e) and at 993 and 968 cm^{-1} for HR (f). For the BR spectrum (e), the D_2O-sensitive intense bands at 974 (+) and 957 (+) cm^{-1} were assigned as HOOP vibrations of C15−H and N−H groups (*44*), indicating that the structural changes of BR upon formation of the K intermediate are localized to the Schiff base region unlike photosensory rhodopsins. Thus, the HOOP modes were highly different between photosensors (Figure 4a−d) and ion-pumps (e, f).

The bands at 864 and 861 cm^{-1} were assigned as C14-HOOP in SRII (Figure 4c) and BR-T (d), respectively, the presence of which is highly correlated with negative phototaxis (*28*). It appears that *Sr*SRI does not possess such a band (Figure 4a). Instead, *Sr*SRI possesses a peak at 803 cm^{-1}, which was absent for SRII and BR-T but present for BR. In the BR spectra (Figure 4e), two intense positive bands at 811 and 803 cm^{-1} are likely to originate from wagging vibrations of the retinal chromophore, because resonance Raman study reported that such vibrations appeared in the 900−800 cm^{-1} region (*45*). Therefore the same band in *Sr*SRI would originate from the vibration, although the band at 803 cm^{-1} is more largely shifted upon D_2O hydration than those in BR.

Figure 5 shows the spectral changes in D_2O in the 2560−1900 cm^{-1} region, which contains O−D and N−D stretching vibrations. The measurements for SRII, BR, and HR are reproduced from the published spectra (*34*−*36*). The bands at 2515 (−)/2474 (+) cm^{-1} of SRII (b) and 2506 (−)/2466 (+) cm^{-1} of BR (c) were previously assigned as the O−D stretch of Thr79 and Thr89, respectively (*46, 47*). Therefore, similar bands at 2526 (−)/2471 (+) cm^{-1} of *Sr*SRI (a) that show no isotope shift of $D_2{}^{18}O$ possibly originate from the O−D stretch of a conserved threonine residue (Thr76) (Figure 1). A low frequency (2526 cm^{-1}) as threonine O−D stretch is an indication of a strong hydrogen bond of Thr76 in *Sr*SRI, presumably with a counterion, Asp72. A lower frequency shift from 2526 to 2471 cm^{-1} implies a further strengthened hydrogen bond of Thr76 upon retinal photoisomerization.

Some peaks in this frequency region exhibit spectral downshift by ~10 cm^{-1} in $D_2{}^{18}O$ (blue spectra in Figure 5), which originate from O−D stretching vibrations of water molecules. Proton-pumping rhodopsins possess strongly hydrogen-bonded water molecule(s), whose O−D stretch is located at <2400 cm^{-1} (*48*). The water stretches of SRII at 2307 and 2215 cm^{-1} (Figure 5b) and those of BR at 2323, 2292, and 2171 cm^{-1} (Figure 5c) correspond to strongly hydrogen-bonded water molecules (*16, 17*). HR has only moderately hydrogen-bonded water molecules at 2535, 2501, and 2445 cm^{-1} in the unphotolyzed state, though retinal isomerization strengthens the water hydrogen bond as shown at 2384 and 2263 cm^{-1} (Figure 5d) (*36*). In the case of *Sr*SRI, a strongly hydrogen-bonded water molecule was observed at 2172 cm^{-1} (Figure 5a). In addition, water bands were

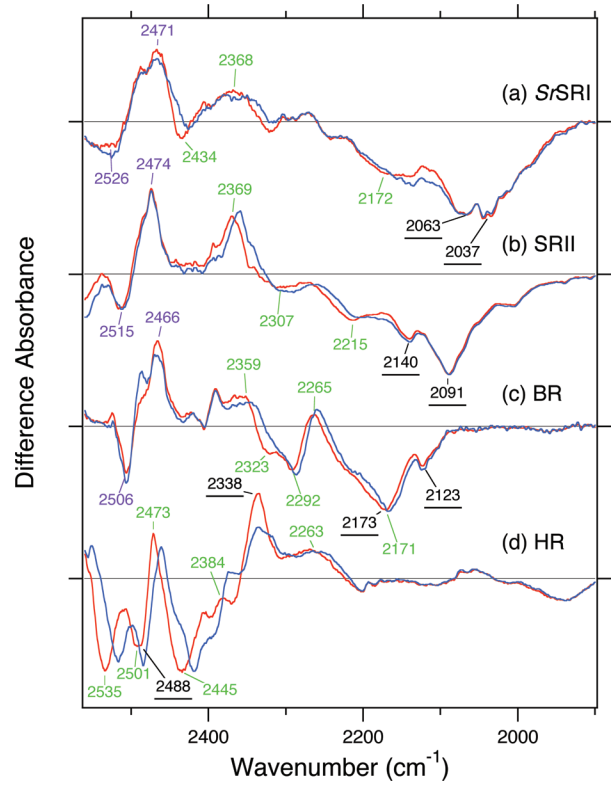

FIGURE 5: *Sr*SRI$_K$ minus *Sr*SRI (a) difference infrared spectra measured at pH 7.0 in the 2560−1900 cm^{-1} region. The samples were hydrated with D_2O (red line) and with $D_2{}^{18}O$ (blue line). Underline, green label, and purple label correspond to C=N stretching vibration, vibration of water molecules, and vibration of threonine residue, respectively. The SRII$_K$ minus SRII (b), BR$_K$ minus BR (c), and HR$_K$ minus HR (d) difference FTIR spectra are reproduced from refs *34*, *35*, and *36*, respectively, for comparison. One division of *y* axis corresponds to 0.0012 absorbance units.

observed at 2434 (−)/2368 (+) cm^{-1} (Figure 5a), as well as 2651 and 2611 cm^{-1} (data not shown).

The peaks at 2063 and 2037 cm^{-1} in *Sr*SRI (Figure 5a) do not originate from the water O−D stretch. The peaks at 2140 and 2091 cm^{-1} in SRII (b) and those at 2173 and 2123 cm^{-1} in BR (c) were previously assigned to the N−D stretches of the Schiff base, using ^{15}N-Lys containing proteins (*47, 49*). Therefore, the 2063 and 2037 cm^{-1} bands in *Sr*SRI are good candidates for the Schiff base vibration. Lower frequencies of these bands indicate that hydrogen-bonding strength of the N−D group in *Sr*SRI is stronger than those of BR and SRII, which is consistent with the analysis of C=N stretching vibrations (Figure 3) (*34, 35*).

Infrared Spectral Changes of SrSRI, HsSRI, and SRII upon Formation of M Photointermediate. Figure 6a shows the M minus initial state difference FTIR spectra of *Sr*SRI (a). Difference FTIR spectra for *Hs*SRI (b) and SRII (c) are reproduced from refs *32* and *39*, respectively, for comparison. The bands at 1525 (−)/1562 (+) cm^{-1} for *Sr*SRI, 1525 (−)/1559 (+) cm^{-1} for *Hs*SRI, and 1545 (−)/1568 (+) cm^{-1} for SRII correspond to the ethylenic C=C stretching vibrations of the retinal chromophore, but amide-II vibrations also possibly appear. In fact, resonance Raman data reported the C=C stretches of the M state of *Hs*SRI at 1568 cm^{-1} (*31*), not at 1559 cm^{-1}. Negative bands at 1249, 1199, and 1164 cm^{-1} for *Sr*SRI are attributable to the C−C stretching vibration of the retinal chromophore, where intensity of the corresponding positive bands is much reduced because of

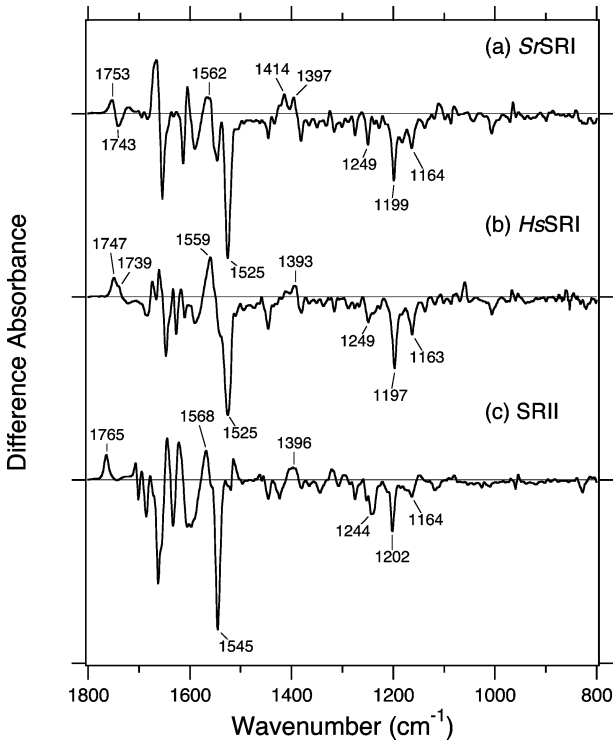

FIGURE 6: *Sr*SRI$_M$ minus *Sr*SRI (a) difference infrared spectra measured at 260 K at pH 7.0 in the 1800−800 cm^{-1} region. The samples were hydrated with H_2O. The *Hs*SRI$_M$ minus *Hs*SRI (b) and SRII$_M$ minus SRII (c) difference FTIR spectra are reproduced from refs *32* and *39*, respectively, for comparison. One division of *y* axis corresponds to 0.01 absorbance units.

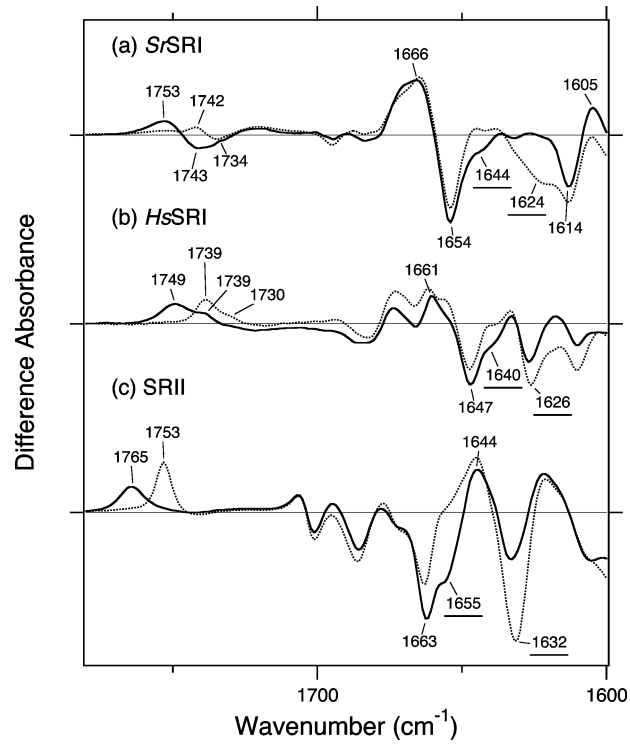

FIGURE 7: *Sr*SRI$_M$ minus *Sr*SRI (a) difference infrared spectra measured at 260 K at pH 7.0 in the 1780−1600 cm^{-1} region. The samples were hydrated with H_2O (—) or D_2O (•••). Underlined values corresponds to C═N stretching vibration. The*Hs*SRI$_M$ minus *Hs*SRI (b) and SRII$_M$ minus SRII (c) difference FTIR spectra are reproduced from refs *32* and *39*, respectively, for comparison. One division of *y* axis corresponds to 0.01 absorbance units.

deprotonation of the Schiff base. All three spectra show a positive peak at 1397−1393 cm^{-1}. In addition, the *Sr*SRI$_M$ minus *Sr*SRI spectrum shows an additional peak at 1414 cm^{-1} (Figure 6a). Since COO^- stretching vibrations of carboxylate appear in this frequency region, the positive band may correspond to deprotonation of a protonated carboxylic acid at 1743 cm^{-1}.

Figure 7 shows the spectral changes in the 1780−1600 cm^{-1} region. When the Schiff base counterion (Asp72 for *Sr*SRI; Asp76 for *Hs*SRI; Asp75 for SRII) is deprotonated, the M formation accompanies a proton transfer from the Schiff base to the counterion. The experimental conditions are indeed the cause, because the pH is higher than the pK_a of the counterion. In SRII, the positive band at 1765 cm^{-1} in H_2O and at 1753 cm^{-1} in D_2O represents the protonation signal of Asp75 (Figure 7c) (*39*). In *Hs*SRI, the positive band at 1749 cm^{-1} band in H_2O and at 1739 cm^{-1} in D_2O were assigned as the C═O stretching vibration of Asp76 (Figure 7b) (*30, 32*). In the case of *Sr*SRI, we observed a positive band at 1753 cm^{-1} in H_2O, which shifts to 1742 cm^{-1} in D_2O (Figure 7a). Therefore, it is reasonable to assign the band as the C═O stretching vibration of Asp72.

Interestingly, the *Sr*SRI$_M$ minus *Sr*SRI spectrum exhibits an additional negative band at 1743 cm^{-1} in H_2O, shifting to 1734 cm^{-1} in D_2O. At present, we cannot exclude the possibility that the bands at 1753 (+)/1743 (−) cm^{-1} originate from a carboxylic acid (hydrogen-bonding alteration of a protonated carboxylic acid), but it is unlikely because the M formation probably accompanies a proton transfer to Asp72. Thus, a protonated carboxylic acid undergoes deprotonation upon formation of the M intermediate. A positive band at 1414 cm^{-1} (Figure 6a) possibly corresponds to the signal of the carboxylate deprotonation. In BR, the M formation accompanies proton release from a protonated water cluster, not from a carboxylic acid (*22, 23*). The present observation may indicate proton release from a carboxylic acid at the extracellular side of *Sr*SRI, which is also the case in some BR mutants (*50*).

Figure 7 shows the C═N stretching vibrations in H_2O and D_2O: at 1644 and 1624 cm^{-1} in *Sr*SRI (a), at 1640 and 1626 cm^{-1} in *Hs*SRI (b), and at 1655 and 1632 cm^{-1} in SRII (c), respectively. On the other hand, H/D-insensitive bands can be identified as an amide-I vibration. Figure 7 shows such bands at 1666 (+)/1654 (−) cm^{-1} for *Sr*SRI (a), at 1661 (+)/1647 (−) cm^{-1} for *Hs*SRI (b), and at 1663 (−)/1644 (+) cm^{-1} for SRII (c), which correspond to an amide-I vibration of the α-helix. Interestingly, frequency shifts were opposite between SRI and SRII, where a downshift and an upshift were observed, respecively. This indicates that the M formation accompanies a weakened hydrogen bond of the α-helix in SRI but a strengthened hydrogen bond of the α-helix in SRII. In other words, activation of SRI or SRII may involve breakage or formation of the helical structure.

Figure 8 shows the spectral changes in D_2O in the 2740−1900 cm^{-1} region. Difference FTIR spectra for SRII (b) and BR (c) are reproduced from refs *39* and *38*, respectively, for comparison. The bands at 2704 (+), 2690 (−), and 2640 (+) cm^{-1} in the *Sr*SRI$_M$ minus *Sr*SRI spectrum (Figure 8a) can be identified as water O−D stretching vibrations, whereas no isotope effect of water molecules was observed at <2500 cm^{-1}. Absence of the negative 2172 cm^{-1} band (Figure 5a) in Figure 8a indicates that the strongly

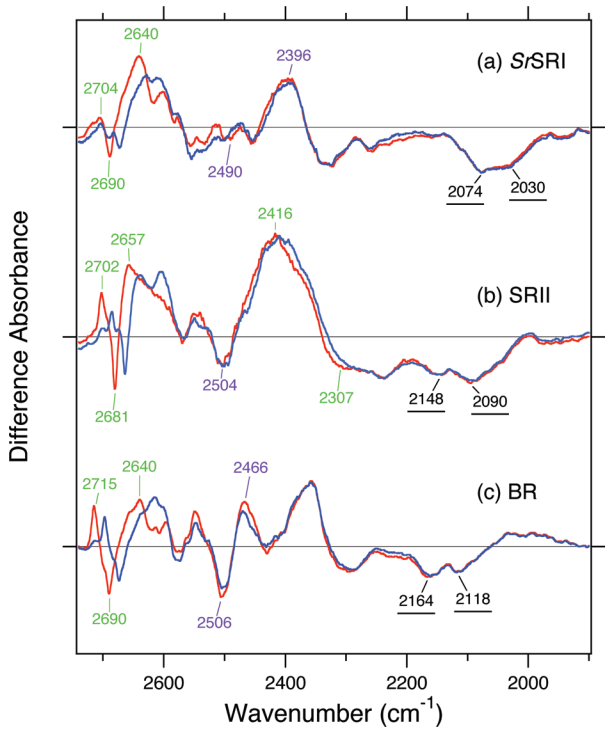

FIGURE 8: *Sr*SRI$_M$ minus *Sr*SRI (a) difference infrared spectra measured at 260 K at pH 7.0 in the 2760−1900 cm^{-1} region. The samples were hydrated with D_2O (red line) and with $D_2{}^{18}O$ (blue line). Underline, green label, and purple label correspond to C═N stretching vibration, vibration of water molecules, and vibration of threonine residue, respectively. The SRII$_M$ minus SRII (b) and BR$_M$ minus BR (c) difference FTIR spectra are reproduced from refs *39* and *38*, respectively, for comparison. One division of *y* axis corresponds to 0.0012 absorbance units.

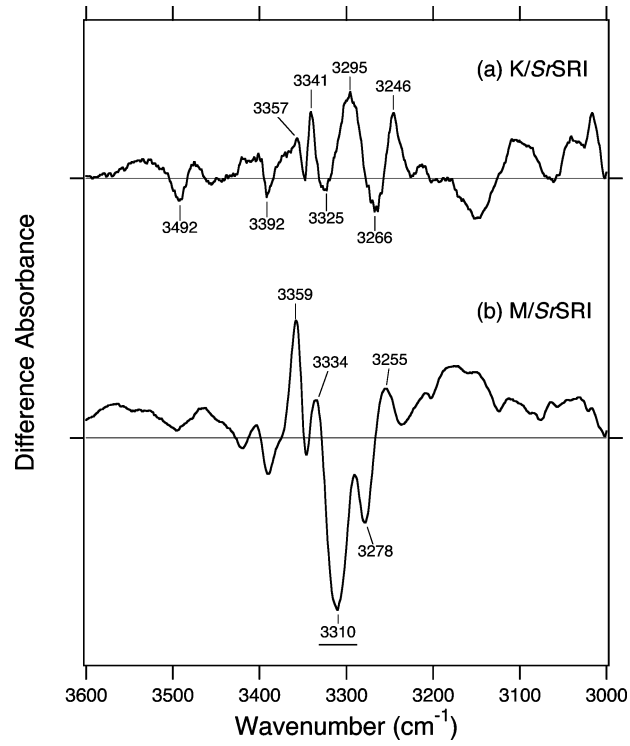

FIGURE 9: *Sr*SRI$_K$ minus *Sr*SRI (a) and *Sr*SRI$_M$ minus *Sr*SRI (b) difference infrared spectra in the 3600−3000 cm^{-1} region, which are multiplied by 1 and 0.66 from Figure 2a and Figure 6a, respectively, to exhibit the same negative intensities at 1250 and 1200 cm^{-1}. Underlined value corresponds to amide-A vibration. One division of *y* axis corresponds to 0.0015 absorbance units.

hydrogen-bonded water molecule in *Sr*SRI restores its hydrogen-bonding strength upon formation of the M intermediate. This is also the case for strongly hydrogen-bonded water molecules in BR (2323, 2292, and 2171 cm^{-1} bands in Figure 5c) and SRII (2215 cm^{-1} band in Figure 5b), but only the negative water band at 2307 cm^{-1} in SRII changes its hydrogen bond in SRII$_M$, presumably shifting to 2416 cm^{-1} (Figure 8b).

The negative bands at 2148 and 2090 cm^{-1} in SRII (Figure 8b) and at 2164 and 2118 cm^{-1} in BR (c) were assigned to the N−D stretch of the Schiff base (*38, 51*). Similar bands were observed at 2074 and 2030 cm^{-1} in *Sr*SRI (Figure 8a), whose frequencies are similar to those in the *Sr*SRI$_K$ minus *Sr*SRI spectrum (Figure 5a). Therefore it is likely that the bands originate from the N−D stretch of the Schiff base. There are also bands at 2504 (−) cm^{-1} in SRII (Figure 8b) and at 2506 (−) and 2466 (+) cm^{-1} in BR (c), which were assigned as the O−D stretch of Thr79 and Thr89, respectively (*46, 47*). Similarly, the bands at 2490 (−) and 2396 (+) cm^{-1} in *Sr*SRI could originate from the O−D stretch of Thr76.

Figure 9 shows the infrared spectra of the *Sr*SRI$_K$ minus *Sr*SRI (a) and *Sr*SRI$_M$ minus *Sr*SRI (b) in D_2O in the 3600−3000 cm^{-1} region, where H/D unexchangeable O−H and N−H stretching vibrations appear. The candidates are N−H stretching vibrations of the peptide backbone (amide-A) and O−H or N−H stretching vibrations of threonine, tyrosine, and tryptophan. In the case of SRII, transducer-dependent bands were observed at 3479 (−)/3369 (+) cm^{-1}, and a mutation study revealed the bands to have originated from an O−H stretch of Thr204 (*26*). Interestingly, importance of Thr204 for negative phototaxis was revealed after the FTIR observation (*20*). Thus, the high-frequency region contains rich structural information related to function. In the *Sr*SRI$_K$ minus *Sr*SRI spectrum, the bands at 3492 (−), 3392 (−), and 3357 (+) cm^{-1} would originate from O−H stretching vibrations of threonine, tyrosine, or tryptophan residue(s).

The N−H stretching vibrations of the peptide backbone (amide-A) also appear in this frequency region. Since N−H and C═O groups form hydrogen bonds in the α-helix, we expect a similar spectral feature for the amide-A and amide-I regions, respectively, and this is indeed the case for the *Sr*SRI$_M$ minus *Sr*SRI spectrum. Figure 9b shows peaks at 3359 (+), 3334 (+), 3310 (−), 3278 (−), and 3255 (+) cm^{-1} in the amide-A region, while Figure 7a shows peaks at 1666 (+), 1654 (−), 1614 (−), and 1605 (+) cm^{-1} in the amide-I region. Thus, negative bands at 3310 and 1654 cm^{-1} correspond with each other in the α-helix, and the M formation accompanies distortion of the α-helix as shown by the upshift to 3359 or 3334 cm^{-1} and 1666 cm^{-1}, respectively. On the other hand, negative bands at 3278 and 1614 cm^{-1} also correspond with each other, and the M formation leads to the spectral downshift. Unlike the former case, the secondary structure is unclear from the frequencies, where *Sr*SRI may form a β-sheet, or some unusual structure.

DISCUSSION

Many organisms utilize light as a signal. SRI is one of the most interesting photosensory receptors because of its ability to mediate opposite signals depending on the color

of light by use of photochromic reactions. However, the molecular mechanism for its function is not well understood at the atomic level. Recently we successfully prepared SRI from a eubacteria source (*Salinibacter ruber*) for the first time (to date found only in the haloarchaea). Most importantly, the *Sr*SRI protein is stable even in the absence of NaCl and amenable to study, unlike SRI from other sources (*10*). Here, we utilized FTIR spectroscopy to explore structural changes of *Sr*SRI and focused on similarities and dissimilarities between *Sr*SRI and other rhodopsins to determine what are important structural changes for function of SRI.

The archaeon *Halobacterium salinarum*, a halophilic prokaryote, contains four retinal proteins, BR, HR, SRI, and SRII. The high-resolution crystal structures of BR, HR, and SRII and the SRII−HtrII complex were reported from 1997 through 2006 (*5, 15, 52, 53*), whereas the structure of SRI has not been determined yet. While high stability of *Sr*SRI (*10*) could lead to crystallization in the future, we will discuss similarities and dissimilarities between *Sr*SRI and other rhodopsins based on the present FTIR observations.

Similarities and Dissimilarities in the Initial State. Protein functions are entirely different among BR (proton pump), HR (chloride pump), and SRII (negative phototaxis sensor), but their X-ray crystallographic structures are very similar among them (*5, 15, 52, 53*). Thus, it is reasonable to infer that SRI has a similar protein architecture to other archaeal-type rhodopsins. The present FTIR study indeed provides this aspect, though FTIR spectroscopy cannot determine the tertiary structure. Similar retinal bands such as C═C and C−C stretching vibrations in *Sr*SRI and *Hs*SRI (Figure 2) to other rhodopsins imply a similar chromophore structure in SRI. Negative amide-I bands at 1654 and 1647 cm^{-1} for *Sr*SRI and *Hs*SRI (Figure 7), respectively, are characteristic of the α-helix, and absolute IR spectrum of *Sr*SRI has a peak at 1657 cm^{-1} (data not shown). Thus, SRI probably possesses an all-*trans* retinal chromophore in seven transmembrane α-helices as do BR, HR, and SRII.

A correlation between proton pumping activity and existence of strongly hydrogen-bonded water molecule(s) (<2400 cm^{-1} as water O−D stretch) was discovered by Kandori's group by using various rhodopsins and their mutants (*48*). Figure 5b,c shows that at <2400 cm^{-1}, there are two water bands for SRII (2307 and 2215 cm^{-1}) and three water bands for BR (2323, 2292, and 2171 cm^{-1}), both of which pump protons. In contrast, strongly hydrogen-bonded water molecules were not observed for HR (Figure 5d), *Neurospora* rhodopsin, and bovine rhodopsin (*17, 36, 54, 55*), which do not pump protons. Figure 5a shows the presence of a water O−D stretch at 2172 cm^{-1} for *Sr*SRI, suggesting proton-pump activity for *Sr*SRI. In fact, light-induced pH changes of the *Sr*SRI-containing vesicles revealed that *Sr*SRI could pump protons as well as BR and SRII (unpublished data). A similar spectrum of *Sr*SRI in the X−D stretching vibrational region to those of BR and SRII (Figure 5), namely, strongly hydrogen-bonded water O−D and Schiff base N−D stretches, also suggest that a water molecule bridges between the Schiff base and Asp72 in *Sr*SRI.

Similarities and Dissimilarities in the K Intermediate. Then, we focused on similarities and dissimilarities in the K intermediate. The $SrSRI_K$ minus *Sr*SRI spectrum is almost identical to that of *Hs*SRI (Figures 2−4), implying a similar structure and structural changes upon formation of the K intermediate between them. It appears that HOOP vibrations are different between photosensors and ion pumps (Figure 4), where HOOP vibrations of SRI and SRII are extended widely along the retinal chromophore. In contrast, the HOOP modes are more localized at the Schiff base region for BR and HR. Spectral analysis of water bands shows that hydrogen-bonding destabilization is important for energy storage in proton pumps, but energy storage for photosensory receptors probably requires a more steric effect, such as a steric constraint between the C14-D group of retinal and Thr204 in SRII (*28*).

In 2008, Ito et al. demonstrated a positive correlation between vibrational amplitudes of the C14−H HOOP vibration at 864 cm^{-1} at 77 K (Figure 4c) and the physiological phototaxis response (*28*). The band was also observable at 861 cm^{-1} for BR-T (Figure 4d), but not for *Sr*SRI (Figure 4a). This suggests that the changes of C14−H HOOP are a specific feature among sensors for negative phototaxis. It is reasonable because the counterpart of the C14 atom, Thr204 of SRII, is not conserved in other rhodopsins, including SRIs. The distortion extended along the polyene chain of the retinal in SRIs may be due to the photoisomerization-induced steric trigger involving the retinylidene C13 methyl group previously demonstrated in *Hs*SRI (*56*), even though the trigger is a different one than in SRII.

The $SrSRI_K$ minus *Sr*SRI spectrum at 3600−3000 cm^{-1} in D_2O (Figure 9a) provides undeuterated O−H or N−H vibrations. Since 2003, Kandori's group have demonstrated that the 110 cm^{-1} upshift of the O−H stretching vibration of Thr204 in SRII and its alteration of hydrogen bond with Tyr174 are required and essential for light-signal transduction to HtrII (*20, 26*). In the case of BR, O−H stretching vibrations of threonine (*57*) and N−H stretching vibrations of tryptophan (*58*) were also studied in detail. Thus, it will be important to identify the bands at 3492, 3392, and 3357 cm^{-1} in Figure 9a, which is one of our future focuses.

Similarities and Dissimilarities in the M Intermediate. Because the active (signaling) intermediate of SRII−HtrII and SRI−HtrI complexes is referred to as the M intermediate (*2*), it is important to analyze the structure and structural changes upon formation of the M intermediate. In the M intermediate, appearance of a protonation signal of the counterion is a common feature among rhodopsins (SRIs, SRII, BR) except for HR, which has no M intermediate (*59*). In *Sr*SRI, the 1753 cm^{-1} band in H_2O (1742 cm^{-1} in D_2O) is ascribable to a C═O stretching vibration of carboxylate (Figure 7a), and interpreted in terms of protonation of Asp72 by the proton transfer from the protonated Schiff base (Lys201) (Figure 10).

In addition, *Sr*SRI has a negative band at 1743 cm^{-1} in H_2O (1734 cm^{-1} in D_2O) (Figure 7a). A corresponding positive peak is observed at 1414 (or 1397) cm^{-1} as a band for deprotonated carboxylate (Figure 6a). Therefore, we infer that in *Sr*SRI, a proton is released from the carboxylate to the extracellular side, although a proton was released from a protonated water cluster in BR (*22, 23*).

The most different aspect between SRI and SRII is the structural changes of the peptide backbone upon formation of the M intermediate (Figures 7 and 9). As described above, the analysis of the M intermediate is important not only for photosensors but also for ion-pumping rhodopsins, because

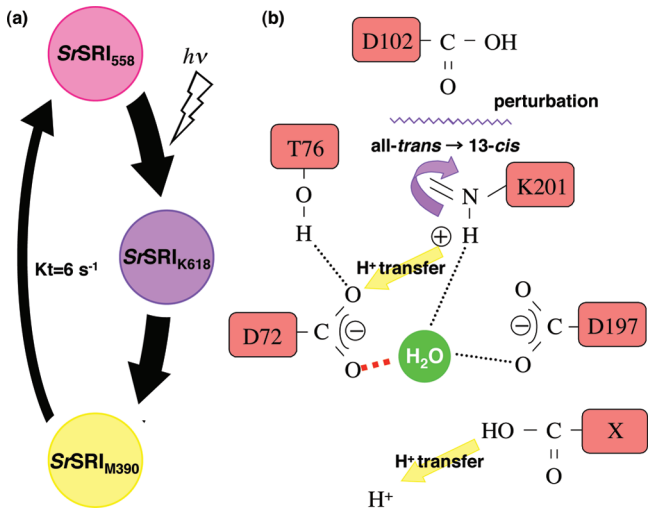

FIGURE 10: (a) Schematic of the photochemical reaction cycle of *Sr*SRI identified in a previous study (*10*). K_t is the decay rate constant of $SrSRI_M$. (b) Structural changes upon formation of K (purple) and M intermediate (yellow). Our results suggest that a strongly hydrogen-bonded water molecule exists between Asp72 and Lys201 in *Sr*SRI. Upon formation of the K intermediate, retinal isomerizes from the all-*trans* to the 13-*cis* form, and Asp102 is affected by the structural changes. The primary proton transfer takes place upon formation of the M intermediate. Then a proton is transferred from the protonated Schiff base (Lys201) to Asp72, and a proton may be released from a carboxylic residue.

of its role on the function. Frequency changes of amide-I vibration of the α-helix were observed at 1666 (+)/1654 (−) cm^{-1} in *Sr*SRI, at 1661 (+)/1647 (−) cm^{-1} in *Hs*SRI, and at 1663 (−)/1644 (+) cm^{-1} in SRII (Figure 7). Namely, these bands in SRIs and in SRII showed a higher and lower frequency shift, respectively. The amide-A vibrations at 3359 (+) and 3334 (+)/3310 (−) cm^{-1} are likely to correspond to the amide-I vibrations at 1666 (+)/1654 (−) cm^{-1}, which probe structural changes in the α-helix. The weakened hydrogen bond of the peptide backbone in SRI is in contrast to those in SRII. The different modes in protein structural changes between SRI and SRII may be correlated with their function, dual receptors both for positive and negative phototaxis versus a receptor for negative phototaxis.

ACKNOWLEDGMENT

We thank Dr. Mikihiro Shibata for providing HR_K minus HR infrared spectra and stimulus discussion, Dr. Jun Sasaki for teaching us the method for preparing film samples of *Hs*SRI suitable for FTIR spectroscopy, and Dr. Tomomi Kitajima-Ihara for encouragement.

REFERENCES

1. Falke, J. J., Bass, R. B., Butler, S. L., Chervitz, S. A., and Danielson, M. A. (1997) The two-component signaling pathway of bacterial chemotaxis: a molecular view of signal transduction by receptors, kinases, and adaptation enzymes. *Annu. Rev. Cell Dev. Biol. 13*, 457–512.
2. Spudich, J. L., and Bogomolni, R. A. (1984) Mechanism of colour discrimination by a bacterial sensory rhodopsin. *Nature 312*, 509–513.
3. Wolff, E. K., Bogomolni, R. A., Scherrer, P., Hess, B., and Stoeckenius, W. (1986) Color discrimination in halobacteria: Spectroscopic characterization of a second sensory receptor covering the blue-green region of the spectrum. *Proc. Natl. Acad. Sci. U.S.A. 83*, 7272–7276.
4. Chen, X., and Spudich, J. L. (2002) Demonstration of 2:2 stoichiometry in the functional SRI−HtrI signaling complex in *Halobacterium* membranes by gene fusion analysis. *Biochemistry 41*, 3891–3896.
5. Gordeliy, V. I., Labahn, J., Moukhametzianov, R., Efremov, R., Granzin, J., Schlesinger, R., Buldt, G., Savopol, T., Scheidig, A. J., Klare, J. P., and Engelhard, M. (2002) Molecular basis of transmembrane signalling by sensory rhodopsin II-transducer complex. *Nature 419*, 484–487.
6. Hoff, W. D., Jung, K. H., and Spudich, J. L. (1997) Molecular mechanism of photosignaling by archaeal sensory rhodopsins. *Annu. Rev. Biophys. Biomol. Struct. 26*, 223–258.
7. Sasaki, J., Phillips, B. J., Chen, X., Van Eps, N., Tsai, A. L., Hubbell, W. L., and Spudich, J. L. (2007) Different dark conformations function in color-sensitive photosignaling by the sensory rhodopsin I-HtrI complex. *Biophys. J. 92*, 4045–4053.
8. Sasaki, J., and Spudich, J. L. (2008) Signal transfer in haloarchaeal sensory rhodopsin- transducer complexes. *Photochem. Photobiol. 84*, 863–868.
9. Sudo, Y., Nishihori, T., Iwamoto, M., Shimono, K., Kojima, C., and Kamo, N. (2008) A long-lived M-like state of phoborhodopsin that mimics the active state. *Biophys. J. 95*, 753–760.
10. Kitajima-Ihara, T., Furutani, Y., Suzuki, D., Ihara, K., Kandori, H., Homma, M., and Sudo, Y. (2008) Salinibacter sensory rhodopsin: Sensory rhodopsin I-like protein from a eubacterium. *J. Biol. Chem. 283*, 23533–23541.
11. Bogomolni, R. A., Stoeckenius, W., Szundi, I., Perozo, E., Olson, K. D., and Spudich, J. L. (1994) Removal of transducer HtrI allows electrogenic proton translocation by sensory rhodopsin I. *Proc. Natl. Acad. Sci. U.S.A. 91*, 10188–10192.
12. Sudo, Y., Iwamoto, M., Shimono, K., Sumi, M., and Kamo, N. (2001) Photo-induced proton transport of *pharaonis* phoborhodopsin (sensory rhodopsin II) is ceased by association with the transducer. *Biophys. J. 80*, 916–922.
13. Kandori, H. (2004) Hydration switch model for the proton transfer in the Schiff base region of bacteriorhodopsin. *Biochim. Biophys. Acta 1658*, 72–79.
14. Luecke, H., Schobert, B., Richter, H. T., Cartailler, J. P., and Lanyi, J. K. (1999) Structure of bacteriorhodopsin at 1.55 Å resolution. *J. Mol. Biol. 291*, 899–911.
15. Luecke, H., Schobert, B., Lanyi, J. K., Spudich, E. N., and Spudich, J. L. (2001) Crystal structure of sensory rhodopsin II at 2.4 angstroms: insights into color tuning and transducer interaction. *Science 293*, 1499–1503.
16. Shibata, M., Tanimoto, T., and Kandori, H. (2003) Water molecules in the schiff base region of bacteriorhodopsin. *J. Am. Chem. Soc. 125*, 13312–13313.
17. Kandori, H., Furutani, Y., Shimono, K., Shichida, Y., and Kamo, N. (2001) Internal water molecules of *pharaonis* phoborhodopsin studied by low-temperature infrared spectroscopy. *Biochemistry 40*, 15693–15698.
18. Muneda, N., Shibata, M., Demura, M., and Kandori, H. (2006) Internal water molecules of the proton-pumping halorhodopsin in the presence of azide. *J. Am. Chem. Soc. 128*, 6294–6295.
19. Shibata, M., Yoshitsugu, M., Mizuide, N., Ihara, K., and Kandori, H. (2007) Halide binding by the D212N mutant of bacteriorhodopsin affects hydrogen bonding of water in the active site. *Biochemistry 46*, 7525–7535.
20. Sudo, Y., Furutani, Y., Kandori, H., and Spudich, J. L. (2006) Functional importance of the interhelical hydrogen bond between Thr204 and Tyr174 of sensory rhodopsin II and its alteration during the signaling process. *J. Biol. Chem. 281*, 34239–34245.
21. Haupts, U., Tittor, J., and Oesterhelt, D. (1999) Closing in on bacteriorhodopsin: Progress in understanding the molecule. *Annu. Rev. Biophys. Biomol. Struct. 28*, 367–399.
22. Rammelsberg, R., Huhn, G., Lubben, M., and Gerwert, K. (1998) Bacteriorhodopsin's intramolecular proton-release pathway consists of a hydrogen-bonded network. *Biochemistry 37*, 5001–5009.
23. Lorenz-Fonfria, V. A., Furutani, Y., and Kandori, H. (2008) Active internal waters in the bacteriorhodopsin photocycle. A comparative study of the L and M intermediates at room and cryogenic temperatures by infrared spectroscopy. *Biochemistry 47*, 4071–4081.
24. Sudo, Y., Yamabi, M., Iwamoto, M., Shimono, K., and Kamo, N. (2003) Interaction of *Natronobacterium pharaonis* phoborhodopsin (sensory rhodopsin II) with its cognate transducer probed by increase in the thermal stability. *Photochem. Photobiol. 78*, 511–516.

25. Sudo, Y., and Spudich, J. L. (2006) Three strategically placed hydrogen-bonding residues convert a proton pump into a sensory receptor. *Proc. Natl. Acad. Sci. U.S.A. 103*, 16129–16134.
26. Sudo, Y., Furutani, Y., Shimono, K., Kamo, N., and Kandori, H. (2003) Hydrogen bonding alteration of Thr-204 in the complex between *pharaonis* phoborhodopsin and its transducer protein. *Biochemistry 42*, 14166–14172.
27. Sudo, Y., Furutani, Y., Wada, A., Ito, M., Kamo, N., and Kandori, H. (2005) Steric constraint in the primary photoproduct of an archaeal rhodopsin from regiospecific perturbation of C-D stretching vibration of the retinyl chromophore. *J. Am. Chem. Soc. 127*, 16036–16037.
28. Ito, M., Sudo, Y., Furutani, Y., Okitsu, T., Wada, A., Homma, M., Spudich, J. L., and Kandori, H. (2008) Steric constraint in the primary photoproduct of sensory rhodopsin II is a prerequisite for light-signal transfer to HtrII. *Biochemistry 47*, 6208–6215.
29. Mironova, O. S., Budyak, I. L., Buldt, G., Schlesinger, R., and Heberle, J. (2007) FT-IR difference spectroscopy elucidates crucial interactions of sensory rhodopsin I with the cognate transducer HtrI. *Biochemistry 46*, 9399–9405.
30. Rath, P., Spudich, E., Neal, D. D., Spudich, J. L., and Rothschild, K. J. (1996) Asp76 is the Schiff base counterion and proton acceptor in the proton-translocating form of sensory rhodopsin I. *Biochemistry 35*, 6690–6696.
31. Haupts, U., Eisfeld, W., Stockburger, M., and Oesterhelt, D. (1994) Sensory rhodopsin I photocycle intermediate SRI380 contains 13-*cis* retinal bound via an unprotonated Schiff base. *FEBS Lett. 356*, 25–29.
32. Furutani, Y., Takahashi, H., Sasaki, J., Sudo, Y., Spudich, J. L., and Kandori, H. (2008) Structural changes of sensory rhodopsin I and its transducer protein are dependent on the protonated state of Asp76. *Biochemistry 47*, 2875–2883.
33. Sudo, Y., Yamabi, M., Kato, S., Hasegawa, C., Iwamoto, M., Shimono, K., and Kamo, N. (2006) Importance of specific hydrogen bonds of archaeal rhodopsins for the binding to the transducer protein. *J. Mol. Biol. 357*, 1274–1282.
34. Kandori, H., Shimono, K., Sudo, Y., Iwamoto, M., Shichida, Y., and Kamo, N. (2001) Structural changes of *pharaonis* phoborhodopsin upon photoisomerization of the retinal chromophore: Infrared spectral comparison with bacteriorhodopsin. *Biochemistry 40*, 9238–9246.
35. Shibata, M., and Kandori, H. (2005) FTIR studies of internal water molecules in the Schiff base region of bacteriorhodopsin. *Biochemistry 44*, 7406–7413.
36. Shibata, M., Muneda, N., Sasaki, T., Shimono, K., Kamo, N., Demura, M., and Kandori, H. (2005) Hydrogen-bonding alterations of the protonated Schiff base and water molecule in the chloride pump of *Natronobacterium pharaonis*. *Biochemistry 44*, 12279–12286.
37. Sudo, Y., Furutani, Y., Spudich, J. L., and Kandori, H. (2007) Early photocycle structural changes in a bacteriorhodopsin mutant engineered to transmit photosensory signals. *J. Biol. Chem. 282*, 15550–15558.
38. Tanimoto, T., Furutani, Y., and Kandori, H. (2003) Structural changes of water in the Schiff base region of bacteriorhodopsin: proposal of a hydration switch model. *Biochemistry 42*, 2300–2306.
39. Furutani, Y., Iwamoto, M., Shimono, K., Kamo, N., and Kandori, H. (2002) FTIR spectroscopy of the M photointermediate in *pharaonis* phoborhodopsin. *Biophys. J. 83*, 3482–3489.
40. Furutani, Y., Sudo, Y., Wada, A., Ito, M., Shimono, K., Kamo, N., and Kandori, H. (2006) Assignment of the hydrogen-out-of-plane and -in-plane vibrations of the retinal chromophore in the K intermediate of *pharaonis* phoborhodopsin. *Biochemistry 45*, 11836–11843.
41. Kandori, H., Shimono, K., Shichida, Y., and Kamo, N. (2002) Interaction of Asn105 with the retinal chromophore during photoisomerization of *pharaonis* phoborhodopsin. *Biochemistry 41*, 4554–4559.
42. Braiman, M. S., Mogi, T., Marti, T., Stern, L. J., Khorana, H. G., and Rothschild, K. J. (1988) Vibrational spectroscopy of bacteriorhodopsin mutants: light-driven proton transport involves protonation changes of aspartic acid residues 85, 96, and 212. *Biochemistry 27*, 8516–8520.
43. Chon, Y. S., Kandori, H., Sasaki, J., Lanyi, J. K., Needleman, R., and Maeda, A. (1999) Existence of two L photointermediates of halorhodopsin from *Halobacterium salinarium*, differing in their protein and water FTIR bands. *Biochemistry 38*, 9449–9455.
44. Maeda, A., Sasaki, J., Pfefferle, J., M., Shichida, Y., and Yoshizawa, T. (1991) Fourier transform infrared spectral studies on the Schiff base mode of all-*trans* bacteriorhodopsin and its photointermediates K and L. *Photochem. Photobiol. 54*, 911–921.
45. Palings, I., van den Berg, E. M., Lugtenburg, J., and Mathies, R. A. (1989) Complete assignment of the hydrogen out-of-plane wagging vibrations of bathorhodopsin: Chromophore structure and energy storage in the primary photoproduct of vision. *Biochemistry 28*, 1498–1507.
46. Kandori, H., Kinoshita, N., Yamazaki, Y., Maeda, A., Shichida, Y., Needleman, R., Lanyi, J. K., Bizounok, M., Herzfeld, J., Raap, J., and Lugtenburg, J. (1999) Structural change of threonine 89 upon photoisomerization in bacteriorhodopsin as revealed by polarized FTIR spectroscopy. *Biochemistry 38*, 9676–9683.
47. Shimono, K., Furutani, Y., Kamo, N., and Kandori, H. (2003) Vibrational modes of the protonated Schiff base in *pharaonis* phoborhodopsin. *Biochemistry 42*, 7801–7806.
48. Furutani, Y., Shibata, M., and Kandori, H. (2005) Strongly hydrogen-bonded water molecules in the Schiff base region of rhodopsins. *Photochem. Photobiol. Sci. 4*, 661–666.
49. Kandori, H., Belenky, M., and Herzfeld, J. (2002) Vibrational frequency and dipolar orientation of the protonated Schiff base in bacteriorhodopsin before and after photoisomerization. *Biochemistry 41*, 6026–6031.
50. Garczarek, F., Brown, L. S., Lanyi, J. K., and Gerwert, K. (2005) Proton binding within a membrane protein by a protonated water cluster. *Proc. Natl. Acad. Sci. U.S.A. 102*, 3633–3638.
51. Furutani, Y., Iwamoto, M., Shimono, K., Wada, A., Ito, M., Kamo, N., and Kandori, H. (2004) FTIR spectroscopy of the O photointermediate in *pharaonis* phoborhodopsin. *Biochemistry 43*, 5204–5212.
52. Pebay-Peyroula, E., Rummel, G., Rosenbusch, J. P., and Landau, E. M. (1997) X-ray structure of bacteriorhodopsin at 2.5 angstroms from microcrystals grown in lipidic cubic phases. *Science 277*, 1676–1681.
53. Kolbe, M., Besir, H., Essen, L. O., and Oesterhelt, D. (2000) Structure of the light-driven chloride pump halorhodopsin at 1.8 Å resolution. *Science 288*, 1390–1396.
54. Furutani, Y., Bezerra, A. G., Jr., Waschuk, S., Sumii, M., Brown, L. S., and Kandori, H. (2004) FTIR spectroscopy of the K photointermediate of *Neurospora* rhodopsin: structural changes of the retinal, protein, and water molecules after photoisomerization. *Biochemistry 43*, 9636–9646.
55. Furutani, Y., Shichida, Y., and Kandori, H. (2003) Structural changes of water molecules during the photoactivation processes in bovine rhodopsin. *Biochemistry 42*, 9619–9625.
56. Yan, B., Nakanishi, K., and Spudich, J. L. (1991) Mechanism of activation of sensory rhodopsin I: evidence for a steric trigger. *Proc. Natl. Acad. Sci. U.S.A. 88*, 9412–9416.
57. Kandori, H., Kinoshita, N., Yamazaki, Y., Maeda, A., Shichida, Y., Needleman, R., Lanyi, J. K., Bizounok, M., Herzfeld, J., Raap, J., and Lugtenburg, J. (2000) Local and distant protein structural changes on photoisomerization of the retinal in bacteriorhodopsin. *Proc. Natl. Acad. Sci. U.S.A. 97*, 4643–4648.
58. Yamazaki, Y., Sasaki, J., Hatanaka, M., Kandori, H., Maeda, A., Needleman, R., Shinada, T., Yoshihara, K., Brown, L. S., and Lanyi, J. K. (1995) Interaction of tryptophan-182 with the retinal 9-methyl group in the L intermediate of bacteriorhodopsin. *Biochemistry 34*, 577–582.
59. Varo, G., Zimanyi, L., Fan, X., Sun, L., Needleman, R., and Lanyi, J. K. (1995) Photocycle of halorhodopsin from *Halobacterium salinarium*. *Biophys. J. 68*, 2062–2072.
60. Olson, K. D., Zhang, X. N., and Spudich, J. L. (1995) Residue replacements of buried aspartyl and related residues in sensory rhodopsin I: D201N produces inverted phototaxis signals. *Proc. Natl. Acad. Sci. U.S.A. 92*, 3185–3189.
61. Zhang, X. N., and Spudich, J. L. (1997) His166 is critical for active-site proton transfer and phototaxis signaling by sensory rhodopsin I. *Biophys. J. 73*, 1516–1523.
62. Jung, K. H., and Spudich, J. L. (1998) Suppressor mutation analysis of the sensory rhodopsin I-transducer complex: Insights into the color-sensing mechanism. *J. Bacteriol. 180*, 2033–2042.

BI801358B